Quantitative investigation of grain boundary sliding in halite rock by SEM in situ testing and full field strains measurements

Ababacar Gaye, Mathieu Bourcier, Eva Heripre, Michel Bornert, Alexandre Dimanov, Jean Raphanel, Karam Sab

QUANTITATIVE INVESTIGATION OF GRAIN BOUNDARY SLIDING IN HALITE ROCK BY SEM *IN SITU* TESTING AND FULL FIELD STRAIN MEASUREMENTS

A. Gaye[1], M. Bourcier[2], E. Héripré[2], M. Bornert[1], A. Dimanov[2], J. Raphanel[2] and K. Sab[1]
[1]Laboratoire Navier, Université Paris Est, CNRS UMR 8205, École des Ponts ParisTech, 77455 Marne la Vallée
[2]Laboratoire de Mécanique des Solides, CNRS UMR 7649, École Polytechnique, 91128 Palaiseau, France
ababacar.gaye@enpc.fr, bourcier@lms.polytechnique.fr, heripre@lms.polytechnique.fr,
michel.bornert@enpc.fr, dimanov@lms.polytechnique.fr, raphanel@lms.polytechnique.fr, karam.sab@enpc.fr

ABSTRACT: An experimental investigation of the deformation mechanisms acting in halite at the scale of its polycrystalline microstructure is presented. Uniaxial compression tests on centimetric samples are performed inside the chamber of a scanning electron microscope and the obtained high definition images are processed by digital image correlation (DIC) routines. A special marking procedure provides an appropriate contrast at microscale. Standard DIC routines qualitatively demonstrate the coexistence of two deformation mechanisms: crystal slip plasticity and grain boundary sliding. A specific post-processing of the DIC-evaluated displacement fields provides a first quantification of the relative contribution of these mechanisms to overall strain and a dependence with grain size can be demonstrated. A modified DIC formulation able to separate intra-grain deformation from interfacial gliding is also proposed for a better quantification and preliminary results are presented. Such data will be of primary interest for the construction of physically-based multiscale models of the mechanical properties of halite, which might be used for security assessment of deep caverns in salt-rock.

1. INTRODUCTION

Halite is a rock forming mineral with industrial and geotechnical applications, such as liquid or gaseous hydrocarbons storage, or more recently, energy storage in the form of compressed air. A large proportion of strategic hydrocarbon reserves are for instance stored in deep salt caverns. Experimental data on the short and long term mechanical behaviour are required for safety assessments of such underground structures. Mechanical constitutive relations currently in use are essentially based on macroscopic laboratory or field investigations, covering a necessarily limited range of time scales and loading conditions [1]. In order to provide some physical foundation to the extrapolation of such data to other conditions, multiscale modelling approaches, taking into account microstructure and actual physical deformation mechanisms are of potential interest. The present work aims at providing qualititave but also quantitative information on the deformation mechanisms active in halite rock at the scale of its polycrystalline microstructure.

To do so, compression tests have been performed on synthetic halite samples in the chamber of a scanning electron microscope (SEM) at room temperature as well as at 350° and the recorded high definition images have been processed by digital image correlation (DIC) routines. Thanks to their high spatial resolution (local strain gauge length below 2 μm for the highest used image magnification) the obtained strain maps clearly demonstrate the existence of two distinct deformation mechanisms: crystal slip plasticity (CSP), with well separated slip bands within the grains, and grain boundary sliding (GBS) at the interfaces between grains. Qualitative observations on samples with various microstructures suggest that CSP is the dominant mechanism (see also [2] on these slip systems), but that GBS is activated to overcome strain incompatibilities between neighbouring grains. Moreover, GBS seems to be more activ in samples with small grains than in samples with larger one, and less active when temperature increases.

The present paper aims at providing a more quantitative evaluation of the relative contribution of these two mechanisms to the overall deformation of the sample. Two approaches are proposed. A simpler one consists in a post-processing of the DIC-evaluated displacement fields with standard routines taking into account the polycrystalline structure of the material within the region of interest (ROI). A more sophisticated one makes use of a modified DIC formulation able to separate intra-grain deformation from interfacial gliding. The material and the overall experimental procedure are briefly described in next section. More information can be found in references [3, 4]. The general concepts underlying the quantitative partitionning of strain into "intragrain" and "interfacial" contribution is outlined in section 3. This naturally lead to the first simpler procedure. Finally the more elaborated approach is described in the last section and preliminary results are given.

2. SEM IN SITU COMPRESSION TESTS ON SYNTHETIC HALITE

The material under investigation is a synthetic halite obtained by hot-pressing high purity commercial sodium chloride powder. An optional subsequent annealing allows to modify grain size. More details on these elaboration routes can be found in [3, 4]. Three types of microstructures have been investigated: a coarse-grained one, with grains ranging from 200 to 500μm in size, a fine-grained one (30 to 80μm) and a bimodal one, in which small grains (about 80 μm) can be found in betwen larger ones (up to 400 μm). Samples investigated in the SEM are parallelepipedic with a typical length of 12 mm and a cross-section of about 6×6 mm. The lateral observation surface is dry polished. The application of DIC principles requires an appropriate local image contrast at the scale of the investiation. As polished halite samples exhibit a rather uniform grey level, an original and simple procedure has been developped to enhance this contrast without modifying the materials properties. It consists in depositing a very thin gold layer (thickness of about 30 nm) by means of standard evaporation routes for surface metallization. The metallized samples are then annealed at 450°C under atmospheric pressure for 24

hours. During annealing, the thin gold film experiences dewetting and micron-sized gold droplets progressively form at the surface of the sample. These marker provide an efficient contrast for DIC investigation at microscale. A high magnification SEM image of these markers is provided in Fig. 1 together with a zoomed detail of a typical SEM image of a set of grains used for the investigation.

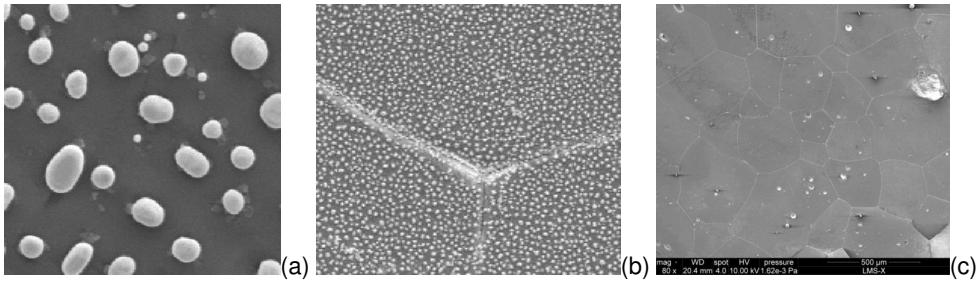

Figure 1 - Gold droplets used as markers on halite sample: observation at high magnification (a), enlarged detail with grain interfaces (b) of a typical SEM image (c) used for DIC analysis, with $\sim$20 grains (coarse-grained material)

Compression tests are performed with a specific test rigg that fits onto the stage of the Field Emission Gun SEM FEI Quanta 600 used in this study. Loading rate is about $8.10^{-5}s^{-1}$. The observation surface is metallized with a thin gold film in order to operate in high vacuum mode with secondary electron imaging. High definition images (4096 $\times$ 3775 pixels) with a sufficiently low noise level are recorded with a dwell time of about 20 s, leading to a total recording time for one image of about 350 s, during which the loading is stopped. A specifically designed oven allows us in addition to heat the sample. Although images are recorded at various magnifications in order to get a multiscale view of the strain field in such materials, the following presentation will be focused on the intermediate magnification with a field of view of about 1.8×1.5mm. An example is shown in Fig. 1c. Note that at such a magnification the marker are slightly too small (about two pixels in the diameter of a microdroplet). About 10 loading stages are considered all along the compression test. Standard DIC routines [5] can be used to process the obtained image sequences. In practice, the in-house code CMV has been used, with typical correlation window sizes of about 10 pixels, a grid step of similar size, an affine local transformation and a bilinear grey level interpolation (no significant difference is observed with biquintic interpolation). As relatively high strain levels are considered in this study (up to 10% macroscopic strain), DIC accuracy is not really an issue, as long as local strain associated with sufficienly large strain gauge length are considered and discontinuities in the displacement field are not considered, and will not be discussed further here. Local and averaged strains are computed according to procedures described in [6].

A typical DIC result in the form of a strain map relative to a local gage length of about 10μm is given in Fig. 2. The overall compression strain is in this case 2% and the 2D von Mises equivalent strain (defined as $2/3(\varepsilon_2 - \varepsilon_1)$ where $\varepsilon_2 > \varepsilon_1$ are the two in-plane principal strains) is plotted; direction of compression is horizontal. A strongly heterogeneous local strain field is observed, with two types of localized deformation bands. The first ones are rectilinear and roughly parallel lines within a single grain and correspond to cristallographic slip planes, through which the displacement is discontinuous. It has been observed that the number of these lines increases with strain. Some grains undergo plasticity at rather low stress level, while other enter into plastic deformation later. The second type of deformation bands are more pronounced but less frequent: they appear at interfaces betwen grains and might not be perfectly rectilinear. They can also be observed at early stages of deformation and new bands are observed when strain increases.

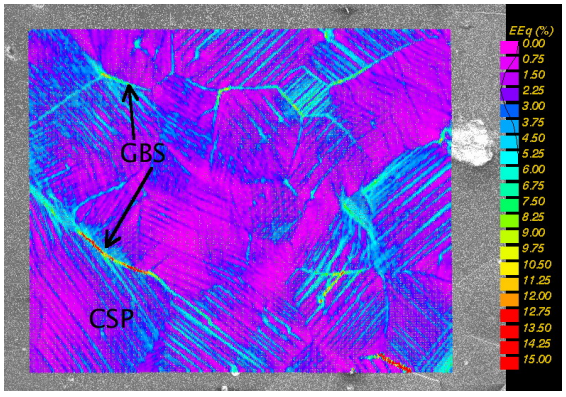

Figure 2 - Typical strain map on a coarse-grained material. Equivalent strain. Two deformation mechanisms are observed. Compression axis is horizontal and average compressive strain is 2%. Local gauge length is 10μm.

The comparison of strain maps observed on several samples tested under various conditions suggests that both mechanisms are required for the overall deformation of halite polycrystals. However CSP seems to be predominant, even if GBS is always present. It also appears that GBS is more generalized (i.e. most interfaces undergo GBS) in fine-grained

sample, and around small grains in bimodal materials. In addition, it seem to be less present at higher temperature, where strain seem to be less heterogeneous (see [4] for details). The following derivations aim at providing tools to quantitatively evaluate the contribution of both mechanisms to the overall strain.

3. STRAIN PARTITIONNING

Let Ω be the domain occupied by the whole ROI, and Ω_g the disjoint surfaces occupied by the G grains g within Ω. In the absence of porosity, one has $\Omega = \cup_{g=1}^{G} \Omega_g$. Let $\omega_g = \|\Omega_g\|/\|\Omega\|$ be the volume fraction of grain g within Ω. Let ξ be the displacement field over Ω.

By definition, the overall deformation gradient over Ω is $\mathbf{F}_\Omega = \mathbf{1} + \frac{1}{|\Omega|}\int_{\partial\Omega} \xi \otimes n \, dl$, where $\mathbf{1}$ is the unit second order tensor and $\partial\Omega$ the boundary of Ω with outward normal n. In case ξ would only be know at discrete positions, as in the case of standard DIC routines, an approximate value of $\mathbf{F}_\Omega$ is obtained by a discretisation of the relation over the available data, and some interpolation assumption. See [6] for the description of the obtained relations in case of a linear interpolation between neighbor measurement positions; these relations are used in CMV. In the case of a regular continuous displacement field, this contour integral can also be transformed into a surface integral involving the local displacement gradient: $|\Omega|(\mathbf{F}_\Omega - \mathbf{1}) = \int_\Omega \nabla\xi \, ds$.

Similar relations can be used to link the overall strain of a grain g to the displacement field at its boundary and the displacement gradient inside it: $|\Omega_g|(\mathbf{F}_{\Omega_g} - \mathbf{1}) = \int_{\Omega_g} \nabla\xi \, ds = \int_{\partial\Omega_p} \xi \otimes n \, dl$. A direct consequence of the overall continuity of ξ is the following classical relation between overall strain and average strains in the grains: $\mathbf{F}_\Omega = \sum_{g=1}^{G} \omega_g \mathbf{F}_{\Omega_g}$. Note that this relation still holds when the displacement field is no longer continuous indide the grains, as in the case of localised crystal plasticity on slip planes, but still continuous at the grain boundaries.

Things are however different when a discontinuity is also observed at the grain interfaces, in which case the displacement to be used to define $\mathbf{F}_{\Omega_g}$ is the displacement at the boundary on the grain side, say ξ_g. One has thus: $|\Omega_g|(\mathbf{F}_{\Omega_g} - \mathbf{1}) = \int_{\partial\Omega_g} \xi_g \otimes n_g \, dl$. Summing up all these relations for the G grains inside the ROI Ω, one gets: $\sum_{g=1}^{G} |\Omega_g|(\mathbf{F}_{\Omega_g} - \mathbf{1}) = |\Omega|(\mathbf{F}_\Omega - \mathbf{1}) + \sum_{g,g'} \int_{\partial\Omega_g \cap \Omega'_g} (\xi_g \otimes n_g + \xi'_g \otimes n'_g) ds$. The last term in this expression spans over all interfaces between grains strictly inside Ω. It does no longer vanish since ξ_g might be different from ξ'_g even though $n_g = -n'_g$. This relation can be reformulated into :

$$\mathbf{F}_\Omega = \sum_{g=1}^{G} \omega_g \mathbf{F}_{\Omega_g} + \frac{1}{|\Omega|}\int_W (\xi^+ - \xi^-) \otimes n) ds = \sum_{g=1}^{G} \omega_g \mathbf{F}_{\Omega_g} + \frac{1}{2}\sum_{g=1}^{G} \frac{1}{|\Omega|}\int_{W \cap \partial\Omega_g} (\xi_g^+ - \xi_g) \otimes n_g) ds \tag{1}$$

where W is the union of all internal interfaces between grains, n its normal with arbitrarily chosen direction, $\xi^+ - \xi^-$ is the displacement jump accross this interface along this direction, and ξ_g^+ the displacement at the boundary of the grain g on the side opposite to the grain.

This relation provides a way to separate the contributions to the overall deformation gradient of intracrystalline phenomena, such as crystal plasticity, and those due to interfacial phenomena such as GBS. The former are provided by the first sum and the second by the last one. Note that the last decomposition in Eq. 1 provides a way to define this strain partitioning at the scale of a single grain. More precisely, the intracrystalline F_g^{Intra} and the interfacial F_g^{Inter} contributions to strain of a grain g will be respectively given by

$$F_g^{Intra} = \mathbf{F}_{\Omega_g} = \int_{\partial\Omega_g} \xi_g \otimes n_g \, dl \qquad F_g^{Inter} = \frac{1}{2}\left(\int_{\partial\Omega_g} \xi_g^+ \otimes n_g \, dl - \int_{\partial\Omega_g} \xi_g \otimes n_g \, dl\right) \tag{2}$$

The question is now to evaluate these quantities from experimental data. The term F_g^{Intra} can be given a first evaluation based on a discretisation of the grains interfaces on the regular grid used for the DIC analysis. In practice, its consists in attributing a "phase index" to each measurement point used in the DIC analysis (either manually, or making use of EBSD data recorded on the same sample an appropriate combination of data). Grain contours "without interface", as defined in [6] and sketched in Fig. 3a, can be constructed and the contour integrals as defined above, provide an evaluation of $\mathbf{F}_{\Omega_g}$. The weighted average of these quantities quantifies the contribution of CSP to overall deformation, while the difference between this result and the average $\mathbf{F}_\Omega$ gives acces to the contribution of GBS. This procedure is a generalisation to multiphase materials of a similar one used by Rupin [7] in the case of two-phase steels. It has been outlined and applied in [3, 4] to various halite samples, and the results confirm the above qualitative observations.

4. MODIFIED DIC PROCEDURE AND POST-PROCESSING

This simple procedure suffers however from two main limitations, clearly illustrated on Fig. 3a . First, used grain contours do not exactly coincide with grain boundaries and a small but non null surface of the ROI is not associated with any grain. The CSP occuring in this "interphase" will then be interpreted as GBS. Second, correlation windows relative to measurement points in these contours might overlap neighbour grains, so that the displacement evaluated at these positions might not be a good evaluation of ξ_g. To overcome these difficulties, a new formulation is proposed. It makes use of similar contour integrals but based on points exactly situated on the grain interfaces. To generate such points, a regular DIC grid is first processed such that points close to an interface are translated exactly onto it (with an accuracy depending on the image

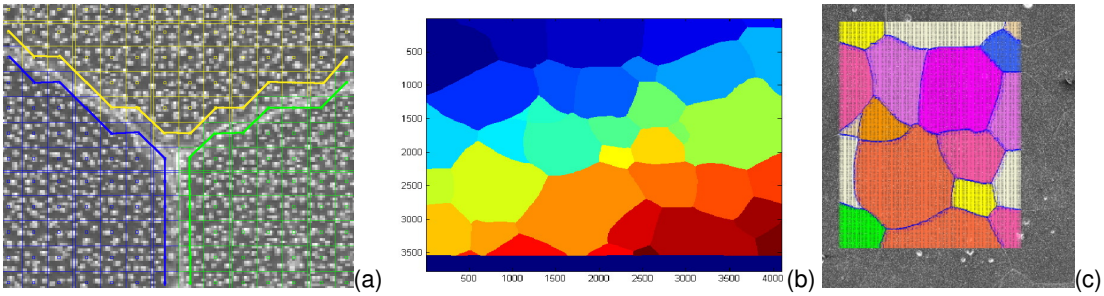

(a) (b) (c)

Figure 3 - Contours used to compute the contribution of intracristalline mechanisms to overall strain, simplified procedure (a). Labelled image (b) used to construct points on the interface (c)

resolution and the interface detection, but no longer on the DIC grid pitch). These points are represented in blue in Fig. 3c. In addition, these points will be attributed two displacements, which are evaluations of ξ_g and ξ_g^+. To do so, DIC algorithms are modified to take into account masks of the reference image, which limit the extension of the correlation windows. These mask are constructed by means of the same labelled image (see Fig. 3b) of the microstructure as the one used to translate points near the interface. When an external mask is used (as in Fig. 4a), image contrast outside grain g is not used and the evaluated displacement will not be perturbated by GBS. On the other hand, an internal mask (Fig. 4c) avoids using information inside grains for the evaluation of the displacement of interfacial points, so that the DIC results is a good estimate of ξ_g^+. The corresponding strain maps (Fig. 4b and d) over the considered grain confirm that grain boundary discontinuities have not been taken into account in the first case, while they generate large strain values at some boundaries of the grain in the second one. Work is under progress to apply this procedure to the experimental data available for various microstructures.

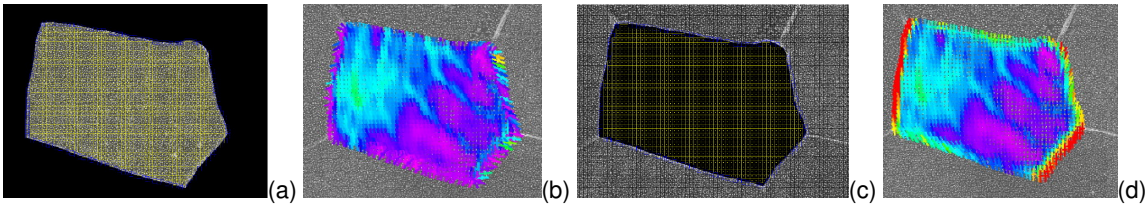

(a) (b) (c) (d)

Figure 4 - Modified image correlation routine: external mask with DIC grid (a) and obtained strain map (b); internal mask (c) and obtained strain map (d) (arbitrary colormap)

5. AKNOWLEDGMENTS

The present work is part of the cooperative project ”MicroNaSel” funded by the Agence Nationale de la Recherche (ANR). Support has also been provided by the chair ”Énergies durables” of Ecole Polytechnique, sponsored by EDF and CEA. The FEG-SEM used in this study has been acquired with the combined financial support of Region Ile de France (”SESAME 2004” program), École polytechnique and CNRS.

6. REFERENCES

1. Bérest, P., Blum, P. A., Charpentier, J. P. Gharbi, H. and Valès , F. (2005) Very slow creep tests on rock samples. *International Journal of Rock Mechanics and Mining Sciences*, 42(4), 569-576.

2. Carter, N. L. and F. Hansen, D. (1983) Creep of rocksalt. *Tectonophysics*, 92(4), 275-333.

3. M. Bourcier, M. Bornert, A. Dimanov, E. Héripré, J. L. Raphanel, (submitted) Grain boundary sliding and crystal plasticity in halite. *Journal of Geophysical Research*

4. M. Bourcier, (2012) Étude multi-échelle des mécanismes de déformation ductiles de polycristaux de chlorure de sodium. PhD thesis, École Polytechnique.

5. Bornert, M., Orteu, J.J., and Roux, S. (2011) Corrélation d’images, in Mesures de champs et identification, Grédiac, M. and Hild, F. Eds., Hermes Science, Chap. 6, 175-208.

6. Allais, L., Bornert, M. Bretheau, T. and Caldemaison, D. (1994) Experimental characterization of the local strain field in a heterogeneous elastoplastic material. *Acta Metallurgica and materialia*, 42(11), 3865-3880.

7. N. Rupin, (2007) Déformation à chaud de matériaux biphasés : modélisations théoriques et confrontations expérimentales, PhD thesis, École Polytechnique.